

The origin of the anomalously strong influence of out-of-plane disorder on high- T_c superconductivity

Y. Okada,¹ T. Takeuchi,² T. Baba,³ S. Shin,³ and H. Ikuta¹

¹*Department of Crystalline Materials, Nagoya University, Nagoya 464-8603, Japan*

²*EcoTopia Science Institute, Nagoya University, Nagoya 464-8603, Japan*

³*Institute for Solid State Physics (ISSP), University of Tokyo, Kashiwa 277-8581, Japan*

(Dated: April 10, 2007)

The electronic structure of $\text{Bi}_2\text{Sr}_{2-x}R_x\text{CuO}_y$ ($R=\text{La, Eu}$) near the $(\pi,0)$ point of the first Brillouin zone was studied by means of angle-resolved photoemission spectroscopy (ARPES). The temperature T^* above which the pseudogap structure in the ARPES spectrum disappears was found to have an R dependence that is opposite to that of the superconducting transition temperature T_c . This indicates that the pseudogap state is competing with high- T_c superconductivity, and the large T_c suppression observed with increasing the out-of-plane disorder is due to the stabilization of the pseudogap state.

High temperature superconductivity occurs with doping carriers to a Mott insulator. Carriers are usually doped either by varying the oxygen content or by an element substitution. Unavoidably, these procedures introduce disorder that influences the superconducting transition temperature T_c although only sites outside the CuO_2 plane are chemically modified. For instance, T_c of the La_2CuO_4 family depends on the size of the cation that substitutes for La [1], and T_c of $\text{Bi}_2\text{Sr}_{1.6}R_{0.4}\text{CuO}_y$ depends on the R element even if the nominal content of R is the same [2, 3]. Recently, some of the present authors have studied extensively the $\text{Bi}_2\text{Sr}_{2-x}R_x\text{CuO}_y$ system using single crystals and varied the R content x over a wide range for $R=\text{La, Sm, and Eu}$ [4]. The results clearly show that T_c at the optimal doping T_c^{max} depends strongly on the R element and decreases with reducing the ionic radius of R , or in other words, with increasing disorder. By plotting T_c as a function of the thermopower at 290 K $S(290)$, it was found that the range of $S(290)$ values for samples with a non-zero T_c becomes narrower with increasing disorder (see Fig. 1). Because $S(290)$ correlates well with hole doping in many high- T_c cuprates [5], this means that the doping range where high- T_c superconductivity occurs is suppressed with increasing disorder [4].

Despite the strong influence on T_c and on the doping width of high- T_c superconductivity, out-of-plane disorder affects the conduction along the CuO_2 plane only weakly. According to Fujita *et al.* [6], out-of-plane disorder suppresses T_c more than Zn when samples with a similar residual resistivity are compared. This means that out-of-plane disorder influences T_c without being a strong scatterer, and that this type of disorder has an unexplained effect on T_c . To elucidate the reason of this puzzling behavior, we studied in this work the electronic structure of $R=\text{La}$ and Eu crystals by means of angle-resolved photoemission spectroscopy (ARPES) measurements. We particularly focused on the so-called antinodal position, the point where the Fermi surface crosses

the $(\pi,0)$ - (π,π) zone boundary (\bar{M} -Y cut), due to the following reasons. It is generally accepted that in-plane resistivity is sensitive to the electronic structure near the nodal point of the Fermi surface [7, 8, 9]. The small influence of out-of-plane disorder on residual resistivity hence suggests that the electronic structure near the nodal region is not much affected by this type of disorder, as Fujita *et al.* already pointed out [6]. Therefore, if out-of-plane disorder causes any influence on the electronic structure, it would be more likely to occur at the antinodal point of the Fermi surface.

The single crystals used in this study were grown by the floating zone method as reported previously [4]. All crystals were annealed at 750°C for 72 hours in air. The ARPES spectra were accumulated using a Scienta SES2002 hemispherical analyzer with the Gammadata VUV5010 photon source (He I α) at the Institute of Solid State Physics (ISSP), the University of Tokyo, and at beam-line BL5U of UVSOR at the Institute for Molecular Science, Okazaki with an incident photon energy of 18.3 eV. The energy resolution was 10-20 meV for all measurements, which was determined by the intensity reduction from 90% to 10% at the Fermi edge of a reference gold spectrum. Thermopower was measured by a four-point method using a home-built equipment.

Figures 2(a) and (c) show the ARPES intensity plots along the $(\pi,0)$ - (π,π) direction (see the arrow in Fig. 2(f)) at 100 K for $R=\text{La}$ and Eu crystals that have a similar hole concentration. The samples were cleaved in situ at 250 K in a vacuum of better than 5×10^{-11} Torr. Thermopower of the crystals that were cleaved from the ARPES samples was measured to determine the doping level. The $S(290)$ values were 4.7 $\mu\text{V}/\text{K}$ and 4.8 $\mu\text{V}/\text{K}$ for the $R=\text{La}$ and Eu samples, respectively, indicating that both samples are slightly underdoped (see Fig. 1) and the doping level is similar. Figures 2(b) and (d) show momentum distribution curves (MDCs) of the $R=\text{La}$ and Eu samples, respectively. We fitted the MDC curves to a Lorentz function to determine the peak position. The

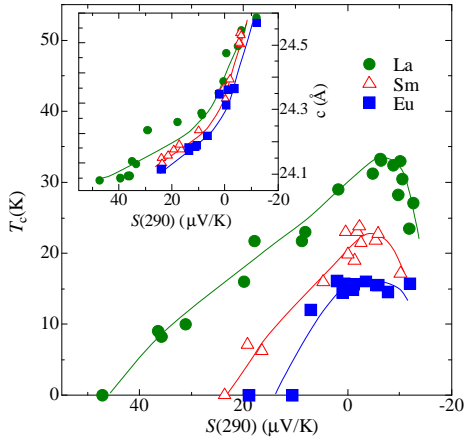


FIG. 1: The critical temperature T_c as a function of $S(290)$, the thermopower at 290 K. T_c was determined from the temperature dependence of resistivity, which was measured simultaneously with thermopower. Data are based on Ref. [4], and some new data points are included. Inset: Lattice constant c plotted as a function of $S(290)$.

thus extracted dispersion is superimposed by white small circles on Figs. 2(a) and (c). The momentum where the dispersion curve crosses the Fermi energy E_F corresponds to the Fermi wave vector k_F on the $(\pi,0)$ - (π,π) cut, and Fig. 2(e) shows the energy distribution curves (EDCs) of the two samples at k_F . Obviously, the $R=La$ sample has a larger spectral weight at E_F than the $R=Eu$ sample, although the doping level of the two samples is very similar.

Figure 3 shows the EDCs of the two samples of Fig. 2 at various temperatures. To remove the effects of the Fermi function on the spectra, we applied the symmetrization method $I_{\text{sym}}(\omega) = I(\omega) + I(-\omega)$, where ω denotes the energy relative to E_F . As shown in Figs. 3(a) and (b), the symmetrized spectra of both samples show clearly a gap structure at the lowest measured temperature, 100 K. Because we are probing the antinodal direction at a temperature that is higher than T_c , we attribute this gap structure to the pseudogap. With increasing the temperature, the gap structure fills up without an obvious change in the gap size. At 250 K, only a small suppression of the spectral weight was observed for the $R=La$ sample. On the other hand, a clear pseudogap structure can be observed for the $R=Eu$ sample even at 250 K. This means that the temperature T^* up to which the pseudogap structure can be observed is certainly different for these two samples despite the closeness of the doping level.

The thin solid lines $I_{\text{fit}}(\omega)$ of Figs. 3(a) and (b) are the results of fitting a Lorentz function to the symmetrized spectrum in the energy range of $E_F \pm 150$ meV. The dashed lines are, on the other hand, the background spectra $I_{\text{bkg}}(\omega)$, which were determined by making a similar fit in the energy range of $150 \text{ meV} \leq |\omega| \leq 400 \text{ meV}$. It can

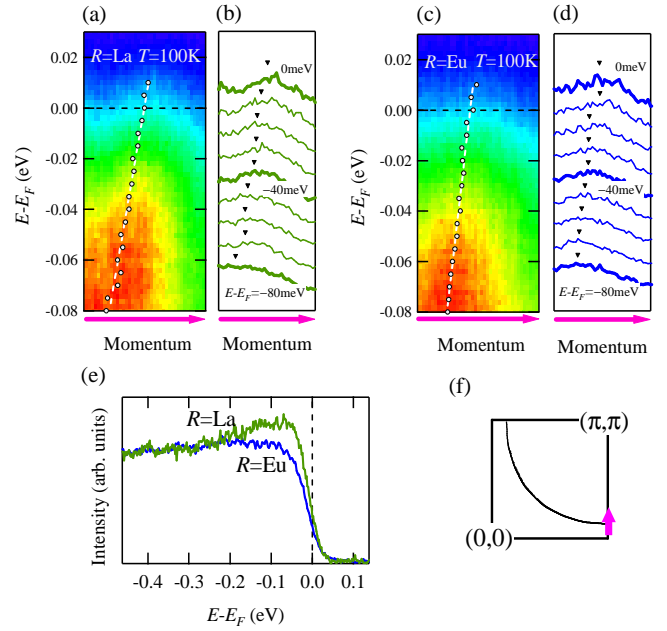


FIG. 2: Intensity plots in the energy-momentum plane of the ARPES spectra at 100 K of slightly underdoped $\text{Bi}_2\text{Sr}_{2-x}\text{R}_x\text{CuO}_y$ samples that have a similar doping level with (a) $R=La$ and (c) $R=Eu$ along the momentum line indicated by the arrow in (f). (b), (d) Momentum distribution curves (MDCs) of the two samples. (e) The energy distribution curves (EDCs) of the two samples at k_F . (f) Schematic drawing of the underlying Fermi surface.

be seen that the difference between the two fitted curves at E_F increases with decreasing the temperature, reflecting the growth of the pseudogap. To quantify how much the spectral weight at the Fermi energy is depressed, we define I_{PG} as the difference between unity and the spectral weight of the fitted spectrum at E_F divided by that of the background curve $(1 - I_{\text{fit}}(0)/I_{\text{bkg}}(0))$. Figure 3(c) shows the temperature dependence of I_{PG} of the two samples. Obviously, the depression of the spectral weight is larger for the $R=Eu$ sample at all measured temperatures, and T^* is higher. I_{PG} is roughly linear temperature dependent for both samples with a very similar slope. Therefore, we extrapolated the data with the same slope as shown by the dashed lines, and estimated T^* to be 282 K and 341 K for the $R=La$ and Eu samples, respectively.

We also measured ARPES spectra of four other samples at 150 K. Assuming that the temperature dependence of I_{PG} is the same as that of Fig. 3(c), we can estimate T^* from the I_{PG} value at 150 K. The thus estimated T^* values are included in Fig. 4(a), which shows T^* of all samples studied in this work as a function of $S(290)$. It can be seen that T^* is higher for $R=Eu$ than $R=La$ when compared at the same $S(290)$ value. Because T_c at the same hole doping decreases with changing the R element to one with a smaller ionic radius (Fig. 1), it is clear that T_c and T^* have an opposite R dependence. This

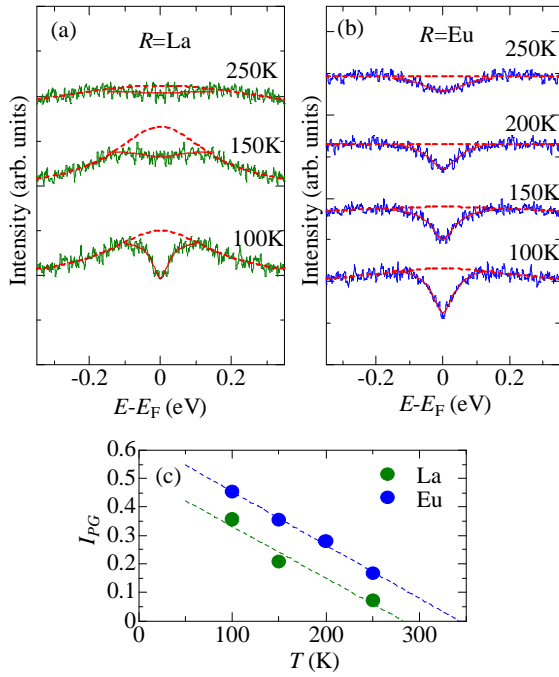


FIG. 3: Temperature dependence of the symmetrized ARPES spectrum at the antinodal point for the (a) $R=\text{La}$ and (b) $R=\text{Eu}$ crystals of Fig. 2. (c) Temperature dependence of the amount of spectral weight suppression I_{PG} .

important finding is summarized on the schematic phase diagram shown in Fig. 4(b) that was drawn based on the data of Figs. 1 and 4(a). As shown, both T_c^{max} and the carrier range where superconductivity takes place on the phase diagram decrease with decreasing the ionic radius of R , while T^* at the same hole concentration increases.

One of the most important issues of pseudogap has been whether such state is a competitive one or a precursor state of high- T_c superconductivity [10]. Figure 4(b) clearly shows that whatever the microscopic origin of the pseudogap is, it is competing with high- T_c superconductivity. In contrast, some other studies have concluded that pseudogap is closely related to the superconducting state because the momentum dependence of the gap is the same above and below T_c and the evolution of the gap structure through T_c is smooth [11, 12, 13]. We point out, however, that several recent experiments revealed the existing of two energy gaps at a temperature well below T_c for underdoped cuprate superconductors [14, 15] as well as for optimally doped $(\text{Bi,Pb})_2(\text{Sr,Lu})_2\text{CuO}_{6+\delta}$ [16]. The energy gap observed in the antinodal region was attributed to the pseudogap while the one near the nodal direction to the superconducting gap. We think that the conffiction encountered in the pseudogap issue arose probably because distinguishing these two gaps would be not easy if their magnitudes were similar.

We next discuss why T_c decreases with the stabilization of the pseudogap state. We think that the ungapped re-

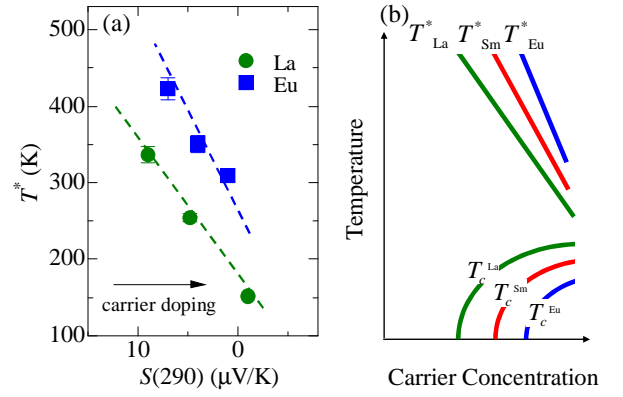


FIG. 4: (a) The pseudogap temperature T^* plotted as a function of $S(290)$. $S(290)$ was determined using the crystal that was cleaved from the one used for ARPES measurements except for the $R=\text{La}$ sample with the largest doping. For that particular sample, the $S(290)$ value was estimated from the c -axis length deduced from x-ray diffraction using the relation between c -axis length and $S(290)$ that is shown in the inset to Fig. 1. (b) A schematic phase diagram of $\text{Bi}_2\text{Sr}_{2-x}\text{R}_x\text{CuO}_y$ based on the results of Figs. 1 and 4(a).

gion on the Fermi surface is smaller for $R=\text{Eu}$ when compared at the same doping and at the same temperature because pseudogap opens at a temperature that is higher than $R=\text{La}$. In other words, the Fermi arc shrinks with changing the R element from La to Eu, which mimics the behavior observed when doping is decreased [8, 17]. Because the superfluid density n_s decreases with underdoping [18], it is reasonable to think that only the states on the Fermi arc can participate to superconductivity. If we think in analogy to the carrier underdoping case, n_s would be smaller for $R=\text{Eu}$ than $R=\text{La}$, and the decrease of T_c is quite naturally explained from the Uemura relation [18].

The faster disappearance of superconductivity with carrier underdoping for $R=\text{Eu}$ (see Fig. 1) is also a straightforward consequence of this model. Moreover, the opening of the pseudogap at the antinodal direction would not increase much the residual in-plane resistivity because the in-plane conduction is mainly governed by the nodal carriers [7, 8, 9]. Hence, the observation that out-of-plane disorder suppresses largely T_c with only a slight increase in the residual resistivity [6] can also be immediately understood. We think that the degree of T_c suppression that comes from the distortion induced in the conduction plane is similar for both Zn and out-of-plane impurities, and can be correlated to the residual resistivity. However, Zn substitution has little influence on the pseudogap state [19], while the latter type of disorder stabilizes the pseudogap state. The enhancement of the pseudogap causes an additional depression of T_c , and out-of-plane disorder has consequently a larger influence on T_c .

As shown in the inset to Fig. 1, the c -axis length de-

terminated by x-ray diffraction from cleaved single crystals decreases in the order of $R=\text{La}$, Sm , and Eu when compared at the same $S(290)$ value. Decrease in the c -axis length with decreasing the ionic size is rather natural, but may be more important than just trivial. It suggests that the distance between Cu and the apical oxygen decreases and/or the CuO_6 octahedra tilt. We expect that the in-plane transfer integrals would decrease in either case, because of the arguments by Pavarini *et al.* [20] for the former case and because a distortion would be induced in the conduction plane for the latter case that reduces the overlap of the wave functions. The effective electron-electron correlation would then increase since the energy cost by Coulomb repulsion against the kinetic energy gain due to planar hopping increases. If the pseudogap state seen in $\text{Bi}_2\text{Sr}_{2-x}\text{R}_x\text{CuO}_y$ were a precursory state of Mott insulator, it is natural to understand that T_c is suppressed and the pseudogap is enhanced with the increase in the effective electron-electron correlation.

Scanning tunneling microscopy/spectroscopy (STM/STS) experiments have revealed a strong inhomogeneity in the local electronic structure that shows up as a spatial distribution in the gap size [21, 22, 23]. The volume fraction of the region with a pseudogap increases with underdoping. The ARPES experiments, on the other hand, show that the spectral weight at the chemical potential of the antinodal region decreases with carrier underdoping [10]. Hence, the antinodal spectral weight at E_F is likely to correlate with the volume fraction of the pseudogap region. Figure 3(c) shows that the spectral weight is lower for the $R=\text{Eu}$ sample when compared at the same hole concentration and temperature. We thus expect that the fraction of superconducting region would be smaller for $R=\text{Eu}$. Indeed, quite recent STM/STS experiments of optimally doped $\text{Bi}_2\text{Sr}_{2-x}\text{R}_x\text{CuO}_y$ report that the averaged gap size increases with changing the R element to one with a smaller ionic radius [24, 25], which can be attributed to the increase of the pseudogapped region. Because n_s can be naturally related to the volume fraction of the superconducting region, the results of STM/STS experiments are consistent with our picture that the stabilization of the pseudogap state decreases superfluid density and suppresses T_c .

In regard to inhomogeneity, it is worthwhile making a comment on the temperature dependence of I_{PG} . Note here that our experimental means is an angle-resolved one and we are not probing the integrated density of states but the spectrum at a particular momentum. Therefore, in an ideal case, the spectral weight at E_F should disappear when a gap opens. Because I_{PG} indicates how much the spectral weight is suppressed at E_F , it is expected that I_{PG} jumps to unity at T^* with no further temperature dependence. The spectra may be broadened because of thermal smearing and instrument resolution. Nevertheless, I_{PG} would still show an

abrupt change at T^* , and would be rather temperature independent at lower temperatures in contrast to the experimental results shown in Fig. 3(c). We think that a reasonable explanation for the observed strong temperature dependence of I_{PG} is that the electronic structure is inhomogeneous and the ARPES spectrum is summing up the electronic structure of regions with different pseudogap size and T^* .

In summary, we have studied the mechanism why T_c^{max} and the carrier range where high- T_c superconductivity occurs depend strongly on the R element in the $\text{Bi}_2\text{Sr}_{2-x}\text{R}_x\text{CuO}_y$ system by investigating the electronic structure at the antinodal direction of the Fermi surface of $R=\text{La}$ and Eu samples. We observed a pseudogap structure in the ARPES spectrum up to a higher temperature for $R=\text{Eu}$ than $R=\text{La}$ when the samples have a similar hole doping, which clearly indicates that the pseudogap state is competing with high- T_c superconductivity. This result suggests that out-of-plane disorder increases the pseudogapped region and reduces the superconducting fluid density, which explains its strong influence on high- T_c superconductivity. We stress that the present results are relevant to all high- T_c superconductors because they are more or less suffered from out-of-plane disorders.

We would like to thank T. Ito of UVSOR and T. Kitao and H. Kaga of Nagoya University for experimental assistance.

-
- [1] J. P. Attfield *et al.*, *Nature* **394**, 157 (1998).
 - [2] H. Nameki *et al.*, *Physica C* **234**, 255 (1994).
 - [3] H. Eisaki *et al.*, *Phys. Rev. B* **69**, 064512 (2004).
 - [4] Y. Okada and H. Ikuta, *Physica C* **445-448**, 84 (2006).
 - [5] S. D. Obertelli *et al.*, *Phys. Rev. B* **46**, 14928 (1992).
 - [6] K. Fujita *et al.*, *Phys. Rev. Lett.* **95**, 097006 (2005).
 - [7] L. B. Ioffe and A. J. Millis, *Phys. Rev. B* **58**, 11631 (1998).
 - [8] T. Yoshida *et al.*, *Phys. Rev. Lett.* **91**, 027001 (2003).
 - [9] T. Yoshida *et al.*, *J. Phys.: Condens. Matter* **19**, 125209 (2007).
 - [10] M. R. Norman *et al.*, *Adv. Phys.* **54**, 715 (2005).
 - [11] H. Ding *et al.*, *Nature* **382**, 51 (1996).
 - [12] Ch. Renner *et al.*, *Phys. Rev. Lett.* **80**, 149 (1998).
 - [13] M. R. Norman *et al.*, *Nature* **392**, 157 (1998).
 - [14] M. Le Tacon *et al.*, *Nature Physics* **2**, 537 (2006).
 - [15] K. Tanaka *et al.*, *Science* **314**, 1910 (2006).
 - [16] T. Kondo *et al.*, *cond-mat/0611517*.
 - [17] K. M. Shen *et al.*, *Science* **307**, 901 (2005).
 - [18] Y. J. Uemura *et al.*, *Phys. Rev. Lett.* **62**, 2317 (1989).
 - [19] A. V. Pimenov *et al.*, *Phys. Rev. Lett.* **94**, 227003 (2005).
 - [20] E. Pavarini *et al.*, *Phys. Rev. Lett.* **87**, 047003 (2001).
 - [21] C. Howald *et al.*, *Phys. Rev. B* **64**, 100504(R) (2001).
 - [22] S. H. Pan *et al.*, *Nature* **413**, 282 (2001).
 - [23] K. M. Lang *et al.*, *Nature* **415**, 412 (2002).
 - [24] A. Sugimoto *et al.*, *Phys. Rev. B* **74**, 094503 (2006).
 - [25] T. Machida, private communication.